# Correlation of Intermolecular Acyl Transfer Reactivity with Noncovalent Lattice Interactions in Molecular Crystals: Toward Prediction of Reactivity of Organic Molecules in the Solid State

Shobhana Krishnaswamy[†] and Mysore S. Shashidhar*

Division of Organic Chemistry, CSIR-National Chemical Laboratory, Pune 411008, India

🅢 Supporting Information

ABSTRACT: Intermolecular acyl transfer reactivity in several molecular crystals was studied, and the outcome of the reactivity was analyzed in the light of structural information obtained from the crystals of the reactants. Minor changes in the molecular structure resulted in significant variations in the noncovalent interactions and packing of molecules in the crystal lattice, which drastically affected the facility of the intermolecular acyl transfer reactivity in these crystals. Analysis of the reactivity vs crystal structure data revealed dependence of the reactivity on electrophile⋯nucleophile interactions and C−H⋯π interactions between the reacting molecules. The presence of these noncovalent interactions augmented the acyl transfer reactivity, while their absence hindered the reactivity of the molecules in the crystal. The validity of these correlations allows the prediction of intermolecular acyl transfer reactivity in crystals and co-crystals of unknown reactivity. This crystal structure−reactivity correlation parallels the molecular structure−reactivity correlation in solution-state reactions, widely accepted as organic functional group transformations, and sets the stage for the development of a similar approach for reactions in the solid state.
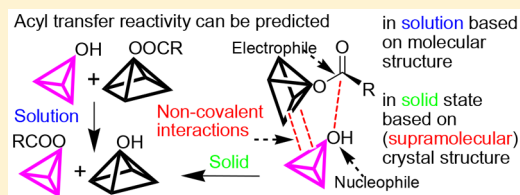
INTRODUCTION

Crystal engineering is the design and construction of molecular solids with desired physical and/or chemical properties, utilizing the principles of molecular recognition, through noncovalent intermolecular interactions.[1] Noncovalent interactions such as hydrogen bonding,[2] halogen bonding,[3] C−H⋯π,[4] halogen⋯halogen,[5] and π⋯π[6] interactions between the appropriate molecular building blocks help in the creation of solids which possess the desired properties or structures for a designated function. However, these interactions are energetically weak and hence competitive, resulting in the formation of other molecular assemblies of comparable energies. The concomitant crystallization of polymorphs and solvates is a consequence of various competitive solute−solute and solute−solvent interactions during the process of nucleation and crystal growth. Therefore, routes for the construction of molecular assemblies of desired structure and/or properties cannot be visualized and realized routinely. This is in contrast to the construction of single molecular entities wherein covalent linkages which are far more stable (compared to noncovalent interactions) at ambient temperature are made. This is obvious when we try to identify the structure of a molecule that is expected to undergo a particular kind of a reaction (the "organic functional group" approach in solution-state reactions) as compared to the identification of a molecular crystal that is capable of undergoing a reaction (in the crystalline state). In other words, it is far more difficult to recognize the chemical reactions that a molecule can undergo in its crystal as compared to its reactions in solution. This is because the reactivity of small organic molecules in fluid phases depends largely on electronic and steric factors within

molecules, while their reactivity in solids is determined largely by packing of (neighboring) molecules. The current article attempts to arrive at parameters that can be used to recognize the ease of acyl transfer reactivity in molecular crystals by a comparison of the crystal structures of several *O*-acylated-*myo*-inositol 1,3,5-orthoesters and the facility of acyl transfer reactivity in these crystals.

The acyl group transfer between oxygen atoms of the same or different molecules is basically a transesterification reaction which involves the addition of the hydroxyl (−OH) group (a nucleophile, Nu) to an ester carbonyl group (an electrophile, El) followed by elimination of a different alcohol (−OH group) leading to the formation of a new ester. If the −OH group being added is that of a water molecule or another alcohol, the reaction is referred to as hydrolysis or alcoholysis, respectively. Acyl transfer reactions have been studied extensively in the solution state since ester hydrolysis and transesterification reactions are ubiquitous in flasks and living cells. Examples of the same reaction are however rare in the crystalline state.[7] We had earlier reported[8] the synthesis and structures of several molecular crystals and co-crystals that exhibit efficient intermolecular acyl transfer reactions (Scheme 1).

There are very few molecular crystals that exhibit efficient reactions (as compared to corresponding reactions in the solution state), hence, they evoke intense interest among chemists.[9] This is mainly because the reactions in crystals exhibit selectivities (regio- as well as stereo-) that are often not possible

Scheme 1. Examples of Intermolecular Acyl Transfer Reactions in the Solid State

Scheme 2. Synthesis of *O*-acylated-*myo*-inositol 1,3,5-orthoesters 8−11
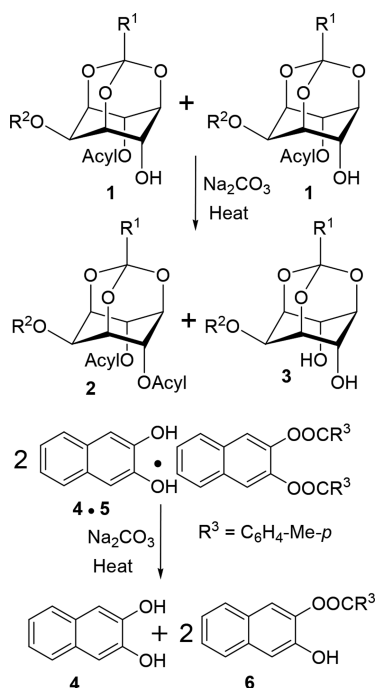
to achieve in solution. The selectivities observed during reactions in crystals are comparable to those observed in enzyme-catalyzed reactions.[10] This is also illustrated by complete enantioselectivity during product formation in crystals comprised solely of achiral molecules.[11] Furthermore, the study of structure of reactive crystals aids in understanding of the corresponding reaction mechanisms and can also help in identification of other crystals that can facilitate similar reactions. The latter possibility, in fact, amounts to the prediction of reactivity of molecular crystals. Reactions in the solid state also have implications for the stability of APIs and drug formulations.[12] The present manuscript describes the correlation of the acyl transfer reactivity with crystal structure and inherent noncovalent interactions of several molecular crystals. This is perhaps the first attempt at systematic correlation of structure and reactivity in molecular crystals for reactions other than addition to C−C multiple bonds.[13] The fact that conclusions arrived at during this analysis allowed us to identify molecular crystals (from a survey of the Cambridge Crystal Structure Database, CSD), which can support intermolecular acyl transfer reactions in them,[8a] establishes the validity of this approach. In a wider perspective, prediction of the structure of possible products in organic reactions is of current interest and relevance to a wide cross section of researchers ranging from chemists to engineers involved in data mining and machine learning.[14]

■ RESULTS AND DISCUSSION

The racemic tosylate **8** was prepared by sequential reaction of the triol **7** with tosyl chloride and benzoyl chloride (Scheme 2). The racemic hydroxyl esters **9**, **10** and **11** were prepared by the *O*-acylation of *myo*-inositol orthoformate **7** with an appropriate acyl chloride. The outcome of these *O*-substitution reactions in the solution state could be predicted based on prior art.[15] All these hydroxyl esters were crystallized from common organic solvents; the crystals obtained were suitable for single crystal X-ray diffraction experiments. Acyl transfer reactivity experiments in
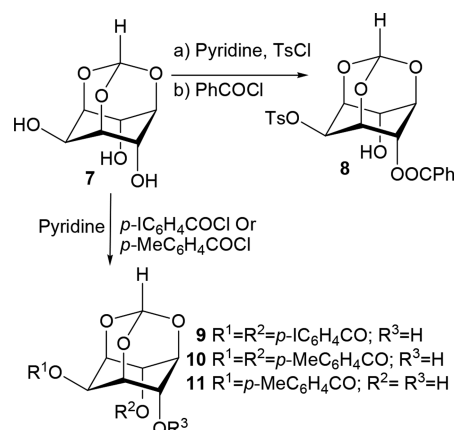
these crystals in the presence of solid sodium carbonate were carried out by experimental procedures developed earlier in our laboratory.[8a]

Assembly of the Molecules in Crystals of 8−11. Glide-related molecules in the crystals of **8** form chains along the *ac*-diagonal through O−H···O hydrogen-bonding interactions which are connected along the *b*-axis by a set of four C−H···O interactions, forming a molecular layer (Figure S21, Table S2, SI). Scrutiny of the molecular assembly revealed that the distance between the nucleophilic (−OH group) and electrophilic (ester C=O group) of adjacent molecules along the *b*-axis is 5.945(4) Å, and the angle between them is 86.63° (Figure 1a). The El···Nu distance is longer than the values observed in crystals that supported acyl transfer reactivity (see below).

Analysis of the organization of molecules in crystals of the *p*-iodo (**9**) and the *p*-methyl (**10**) dibenzoates (Figures S22 and S23, SI) reveal that the hydroxyl group in **9** (and **10**) is engaged in hydrogen bonding with the orthoester oxygen (O4−H4A···O1), forming a homochiral molecular chain along the *a*-axis. Neighboring homochiral molecular chains are linked by C5−H5···O8 contacts and a pair of centrosymmetric C−H···O interactions (C7−H7···O8, C6−H6···O5), forming bilayers (Figures S22a and S23a, Table S2, SI).[16] The bilayers are linked by halogen bonding (C12−I1···O7=C8− of equatorial *p*-iodobenzoate group) interactions in crystals of **9** (Figure S22b, Table S2, SI) while centrosymmetric C−H···π interactions link adjacent bilayers along the *bc*-diagonal in crystals of **10** (Figures S23b, Table S2, SI). Hence, there exists a one-dimensional iso-structurality in these crystal structures. Preference for molecular organization through intermolecular interactions as described above does not bring the hydroxyl group and the ester carbonyl group (El-Nu) in the proximity required for the acyl transfer reaction, in crystals of **9** and **10** (Figure 1b, 1c).

In crystals of the *p*-toluate **11**, adjacent glide related molecules are bound by O4−H4A···O7 (of the *p*-toluate C=O) hydrogen bonds to form a chain (Figure S24a, Table S2, SI). Adjacent antiparallel chains are linked by C13−H13···O1 contacts between the aromatic proton H13 of the *p*-toluate ester and orthoester oxygen O1 along the *ab*-diagonal. The oxygen atom of the second hydroxyl group (O6) forms short O···C=O contacts - El···Nu interactions (O6···C8=O7: 2.909(3) Å, ∠O6···C8=O7: 87.1°) and also engages in C−H···O interactions (C3−H3···O6) with neighboring molecules along the *c*-axis (Figure S24b, Table S2, SI). The promising criteria for acyl transfer reaction in **11** are exhibited by unit translated molecules along the *c*-axis
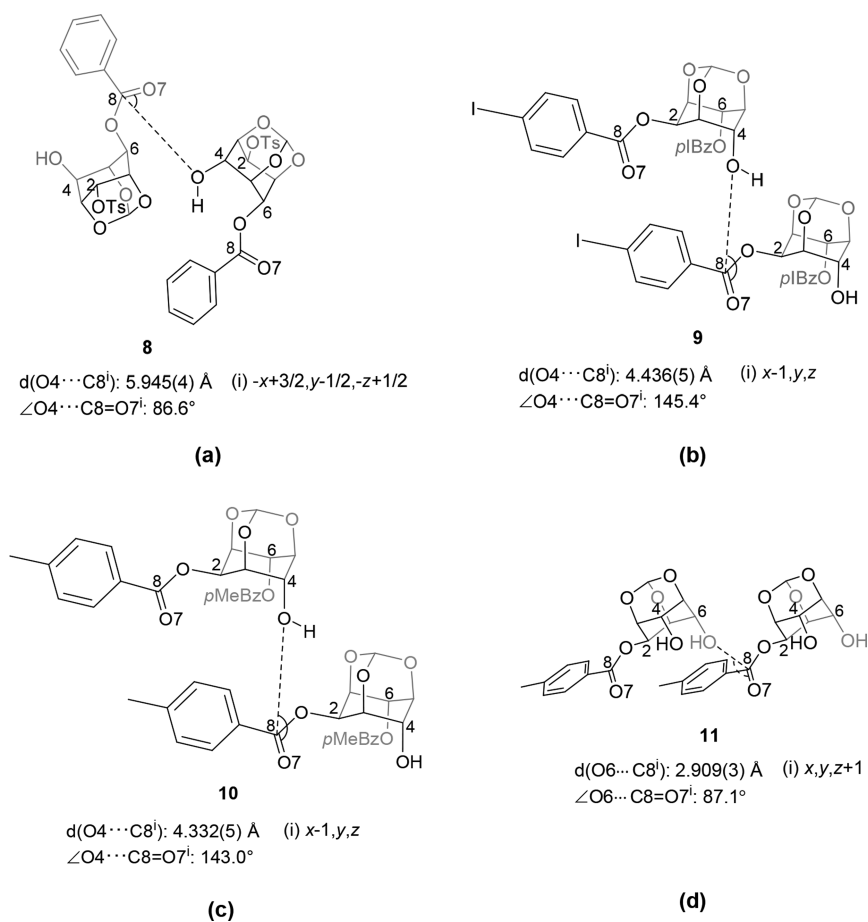
Figure 1. Electrophile-nucleophile geometry observed between neighboring molecules in crystals of **8−11**. These diagrams were generated using the corresponding packing diagrams (Figure S25, SI) obtained with the help of the program 'Mercury 3.8'. Hydrogen atoms other than those of the hydroxyl groups are omitted for clarity.

(Figure 1d). The distance between the potential reaction centers, the nucleophilic O6 and the electrophilic C8=O7, and the corresponding angle of approach are both marginally lesser in magnitude (hence marginally better) than the values observed in reactive crystals.[17] The reactive molecular partners exhibit weak C−H···π interactions between the toluoyl group and the inositol ring H atoms (Figure S24b, SI).[18]

Solid-State Reactivity−Structure Correlation. Heating a mixture of **8** and sodium carbonate below the melting point of racemic **8** led largely to charring of racemic **8**. Analysis of the resulting solid indicated the presence of 2-O-tosyl-4,6-di-O-benzoyl-*myo*-inositol 1,3,5-orthoformate, 2-O-tosyl-*myo*-inositol 1,3,5-orthoformate,[19] and the starting tosylate **8** in low yields. In crystals of **8**, the distance between the nucleophilic (Nu) −OH (O4−H4A) group and the electrophilic ester carbonyl group of the axial benzoate of adjacent molecules along the *b*-axis is (5.945(4) Å) much longer than that observed in the reactive crystals,[17] leading to lower yield of the products, although, the angle of approach, ∠O4···C8=O7 (86.63°) is in the favorable range for acyl transfer reactivity (see below).

While the crystals of the di-p-iodobenzoate **9** reacted in the solid state yielding a mixture of products, the di-p-methylbenzoate **10** was unreactive under similar conditions. The lack of reactivity in these crystals is consistent with molecular organization which does not bring the El-Nu in proximity required for the acyl transfer reaction.
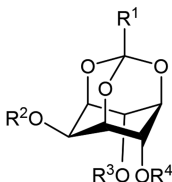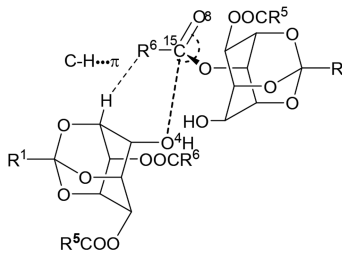
The *p*-toluate diol **11** reacted in the solid state in the presence of sodium carbonate, yielding the diester **10**, the triester **20**, and the triol **7** (Scheme 3). The crystal structure of **11** revealed that

Scheme 3. Acyl Transfer Reactivity in Crystals of 11

7 R^1 = R^2 = R^3 = H
10 R^1 = R^2 = pMeC$_6$H$_4$CO; R^3 = H
20 R^1 = R^2 = R^3 = pMeC$_6$H$_4$CO
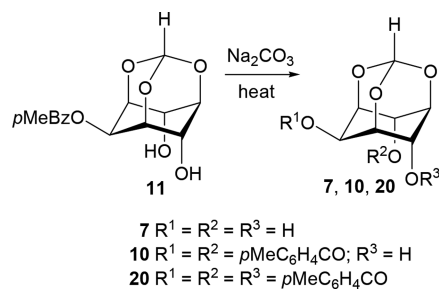
the O6−H6A hydroxyl group makes a short O···C=O contact with the carbonyl carbon C8 of a unit translated molecule along the *c*-axis which is in fact an El−Nu interaction with the distance separating them, 2.909(3) Å, and the angle of approach of Nu toward El, ∠O6···C8=O7, 87.1° (Table 1). These values correspond well with those observed for the reactive dibenzoates **18** and **19**,[17] and the distance between the electrophilic and nucleophilic centers is lesser than the sum of their van der Waals radii. *p*-Toluoyl group transfer is initiated in the presence of the base, and the equatorial ester migrates to the axial position of the next molecule, thereby forming the diester **10** and the triol **7**.

Table 1. Summary of Acyl Transfer Reaction Experiments in Crystals

21 R^1=CH$_3$, R^2=R^3=R^4=C$_6$H$_5$CO
22 R^1=CH$_3$, R^2=C$_6$H$_5$CO, R^3=R^4=H
23 R^1=C$_6$H$_5$, R^2=R^3=R^4=C$_6$H$_5$CO
24 R^1=C$_6$H$_5$, R^2=C$_6$H$_5$CO, R^3=R^4=H
25 R^1=H, R^2=R^3=R^4=C$_6$H$_5$CO

O4···C15=O8 indicates the El···Nu interaction between reacting molecules.

| Entry	Crystals of	Product(s) (%)	El···Nu^a(Å / °)	C–H···π^b(Å / °)
1	**4•5**	**6**(91)	3.166 / 85.6	2.7 / 149; 2.7 / 139
2	**8**	--^{c}	5.945(4) / 86.63	None
3	**9**	--^{c}	4.436(5) / 145.4^e	None
4	**10**	--^{d}	4.332(5) / 143.0^e	None
5	**11**	**7**(39), **10**(29), **20**(8)	2.909(3) / 87.1	2.96 / 159
6	**12**	--^{d}	3.748 / 33.1	None
7	**13**	--^{d}	5.976 / 105.47	None
8	**14**	--^{c}	3.628(2) / 105.6	3.91 / 139
9	**15**	**7**(48), **15**(10), **19**(10)	3.532(2) / 106.1	2.64 / 162
10	**16**	--^{c}	3.533 / 70.21	3.80 / 152
11	**17** Form I	**17**(14), **21**(19), **22**(21)	3.299(2) / 84.01	3.67 / 142
12	**17** Form II	**21**(42), **22**(42)	3.135(4) / 87.6	2.62 / 167
13	**18**	**23**(49), **24**(48)	3.144(2) / 85.6	2.83 / 166
14	**19**	**15**(49), **25**(47)	3.226, 3.249 / 88.1, 89.9	2.53 / 163; 2.62 / 155
15	**17•19**	**15**+**22**(35), **21**+**25**(41)	3.170, 3.155 / 85.9, 88.4	2.66 / 167; 2.59 / 167

^{a}El (O=C)···(OH) Nu distance O4–C15 (Å)/∠O4···C15=O8 (deg) for all crystals except **9**–**11**. O4···C8 (Å)/∠O4···C8=O7 (deg) for **9** and **10**; O6···C8 (Å)/O6···C8=O7 (deg) in **11**, see Figure 1. ^{b}C–H···π interaction between R^6 (or R^5) and a C–H in the adjacent molecule, dist. (Å)/ angle (deg). Crystals in entries 1 and 12−15 had good C–H···π interactions and a well-defined reaction channel for the propagation of the intermolecular acyl transfer reaction. Molecular assembly in other crystals did not result in the formation of well-defined reaction channels. For details of noncovalent interactions in crystals of **8**–**11** see the SI, and **12**, **14**–**17**·**19** see refs 8 and 17. ^{c}Mixture of products, not separated. For experimental details of solid-state reactivity of **12**, **14**–**17**·**19** see refs 8 and 17. ^{d}No reaction. ^{e}El···Nu geometry between the equatorial ester C=O group and hydroxyl group of neighboring molecules ("nearest neighbors" in the crystal structure). In all other crystals El···Nu geometry is between the axial ester C=O group and hydroxyl group of neighboring molecules.

Since molecular packing in crystals of **11** does not support propagation of the reaction in the crystal (as was observed in crystals of the racemic dibenzoate **19**),[17] it appears the reaction occurs in localized pockets in crystals leading to low conversion of reactants to products. It is therefore reasonable to conclude that the lower reactivity observed is a consequence of the absence of a proper channel for the reaction to propagate through the crystal (in spite of excellent El-Nu geometry between the reacting groups in crystals of **11**).

In solid-state reactions, two parameters can be used to judge the efficacy of a reaction: (i) reactivity, the amount of the starting material consumed (more the better), and (ii) selectivity, the number of products formed (lesser the better). We have attempted to correlate both these parameters (see below) with the crystal structures of hydroxyl esters shown in Scheme 4. The extent of acyl transfer reactivity (Scheme 1) in the solid state of

compounds shown in Scheme 2 and their previously reported analogues (Scheme 4) is summarized in Table 1. These compounds were chosen for the study to have a wide variety in molecular structures as well as crystal (supramolecular) structures. These crystalline compounds could be broadly grouped into three categories of reactivity: (a) those that exhibited good and selective intermolecular acyl transfer reactivity; (b) those that exhibited intermolecular acyl transfer reactivity but led to a mixture of products (i.e., nonselective); and (c) those that did not exhibit considerable intermolecular acyl transfer reactivity (i.e., unreactive). Correlation of the crystal structure parameters with the experimentally observed reactivity of the hydroxyl esters in their crystals and co-crystals is presented below.

The variation in the reactivity of hydroxyl esters as a function of the El···Nu geometry is shown in Figure 2. The reactivity is

Scheme 4. Molecular Structure of Hydroxyl Esters Investigated for Intermolecular Acyl Transfer Reactivity in their Crystals[a]
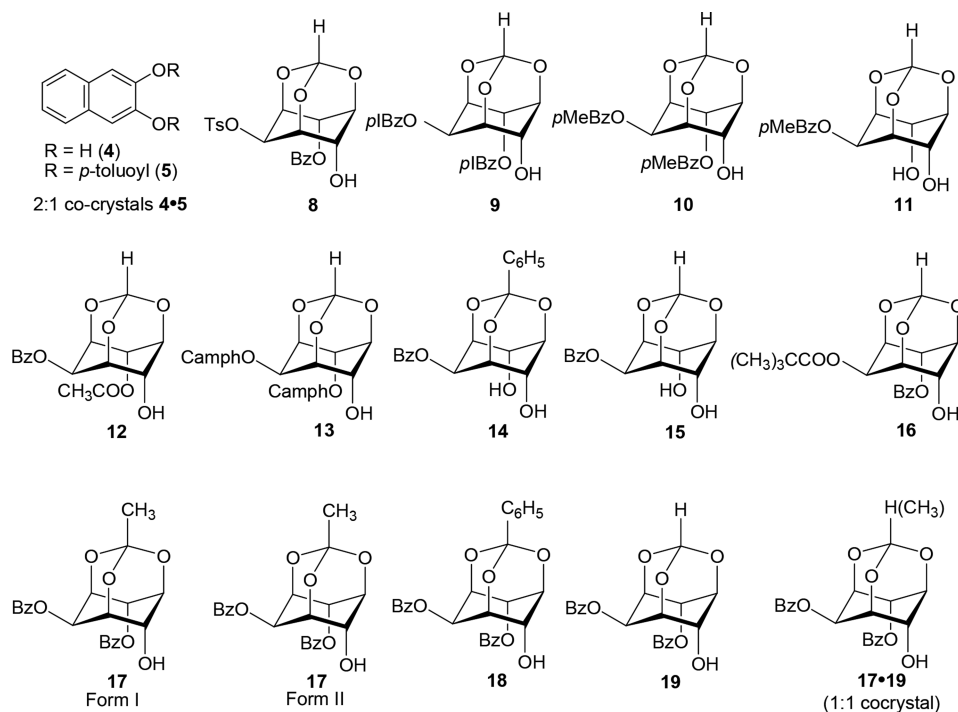
[a]The reactivity of **4·5**, **17** (Form II crystals), **18**, **19**, and **17·19**, was good; reactivity of **8**, **9**, **11**, and **14**−**17** (Form I crystals) was not good, while the esters **10**, **12**, **13**[20] were unreactive. (Camph = camphanoyl).
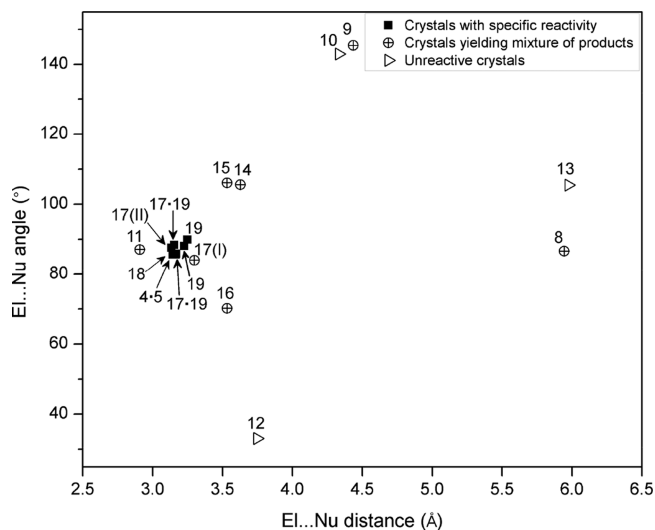

Figure 2. Variation of the acyl transfer reactivity as a function of the El···Nu geometry. Numbers refer to the compounds listed in Table 1.

very good (>90% conversion of hydroxyl ester to expected products by the selective intermolecular migration of the C6−O-acyl group to the C4-hydroxyl group, see cartoon in Table 1), when the El···Nu distance and the angle are close to 3 Å and 85−90° respectively (filled rectangles, Figure 2).[13b] The only exception to this is the 2-p-toluate **11** (circle with cross-wires close to the El···Nu angle-axis of the graph) for which the yield of the product (**10**) based on El···Nu interaction is much <50% (maximum possible for a disproportionation reaction) even though the El···Nu geometry is the best among all the compounds tested. For all other compounds (circles with cross-wires and triangles), the reactivity is low since the El···Nu

geometry deviates from the optimum distance and angle mentioned above (filled rectangles). The exception of 2-p-toluate suggests that El···Nu geometry is not the sole factor that determines the reactivity and selectivity of intermolecular acyl group transfer in crystals of these hydroxyl esters.

The variation in the reactivity of the hydroxyl esters as a function of the C−H···π interactions in their crystals (Figure S26, SI) clearly suggested that crystals which exhibit good reactivity also showed good C−H···π interactions (shorter and linear). This is further supported by a plot of the C−H···π interactions vs the yield of the expected products (Figure 3). This plot shows that the specificity and yield of the acyl transfer reaction is good in crystals that have good C−H···π interactions. These results imply that C−H···π interactions contribute to both reactivity as well as specificity of acyl transfer in crystals of hydroxyl esters. Figure 3 reveals that reactivity of crystals of the 2-p-toluate **11** is not as good as that of dibenzoates **18** or **19** due to the weaker C−H···π interactions (Table 1). A similar effect is also seen by comparison of the reactivity of dimorphs of the orthoacetate dibenzoate **17**.[17d]

A third factor which contributes to the acyl transfer reactivity of crystals under investigation is the presence of reaction channels which help in the propagation of the reaction throughout the crystal in a domino fashion. Such reaction channels are essential since the reaction is initiated by solid sodium carbonate at the surface of crystals, but the acyl transfer reaction must take place throughout the crystal to have high conversion of reactant to products.[17b]

This is clearly established by a comparison of the molecular packing in reactive crystals of dibenzoates **19** and the diol **11** (Figure 4).[17] The p-toluate **11** exhibited a molecular assembly where the reactive centers of unit translated molecules possessed excellent geometry for an acyl transfer reaction. However, a reaction channel for the propagation of the reaction through the
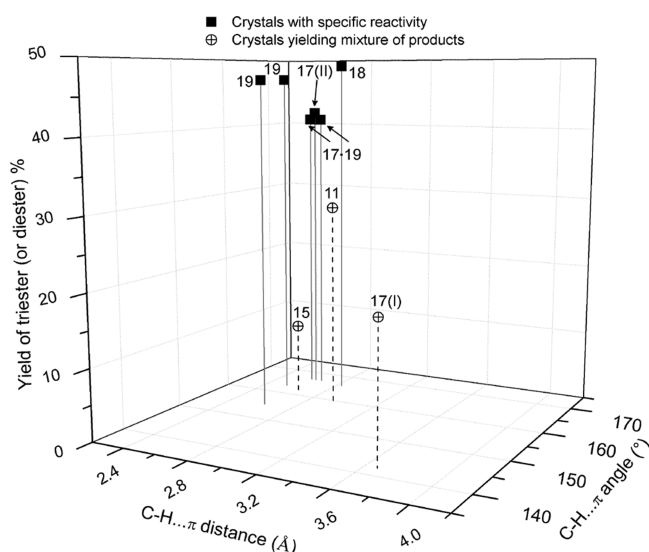
Figure 3. Variation of yield of the triester (diester in case of **11** and **15**) in the solid-state reactions as a function of the C−H⋯π interactions in the crystals. Numbers refer to the compounds listed in Table 1.

crystal was absent, and hence, the solid-state reaction proceeded with less specificity as well as relatively lower yield of the products. The presence of a well-defined reaction channel in a crystal which lacks one or more of the other parameters discussed above, also results in poorer acyl transfer reactivity, as seen in Form I crystals of **17**.[17] It is clear from a comparison of the reactivity and crystal structures of all the hydroxyl esters studied thus far that a crystal which satisfies all the three conditions, viz. (a) the relative geometry of the El and Nu groups with distance

and angle in the neighborhood of 3.2 Å and 90°, respectively; (b) good C−H⋯π interaction which contributes to maintain the topochemical control of the reaction; and (c) presence of channels for the progress of the reaction in the crystal in a domino fashion, exhibits good intermolecular acyl transfer reactivity. In fact, we demonstrated the use of these parameters to identify other crystals from the CSD and verified their reactivity experimentally.[8a] Hence the results presented here show that the crystal (supramolecular) structure−reactivity correlation based on noncovalent interactions presented above is causative and not merely statistical, since absence of any one structural criterion (a−c) in the crystal leads to absence of reactivity.

■ CONCLUSIONS

Investigation of reactions in molecular crystals is a contemporary area of research which has banked heavily on serendipity for the discovery of crystals in which chemical reactions are facile. Solid-state reactions have not been developed to a great extent as a tool in synthetic organic chemistry (as compared to solution-state reactions) barring the exception of photochemical reactions in olefinic crystals, presumably due to the complexity involved in obtaining a suitably preorganized reaction system in the crystalline state.[13b,21] Identification or recognition of reactive molecular crystals is in fact the rate-determining step for the progress in this area of research. Although crystal engineering shows promise of being one of the ways of preparing a reactive molecular crystal, availability of custom designed crystals is still not a reality. The second-best alternative to designing crystals with desired properties (in the present case, reactivity) is to be able to identify reactive crystals from a library of crystal structures. The study and correlation between the solid-state reactivity and the crystal structures of *O*-acyl-*myo*-inositol 1,3,5-
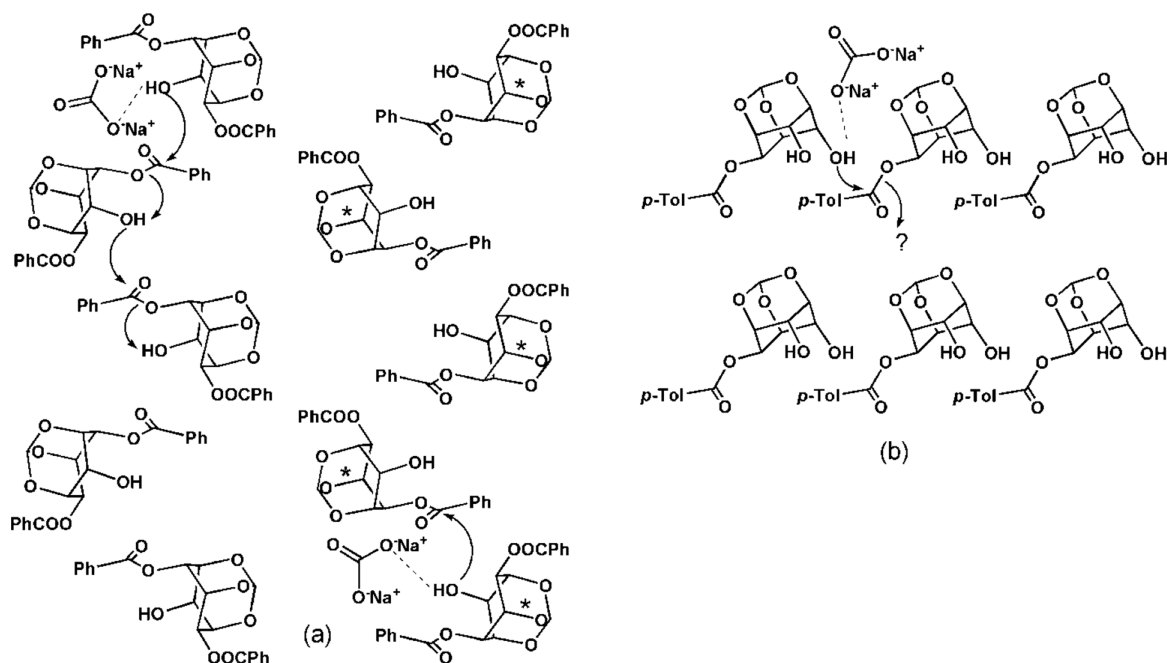

Figure 4. (a) The helical organization of molecules in crystals of racemic **19** provides channels for the propagation of acyl transfer reaction through each helix, resulting in clean reaction and good yield of the products. Sodium carbonate initiates the reaction at one end of each helix; the reaction progresses (as indicated by arrows) along the helix due to successive intermolecular benzoyl group transfer and intramolecular proton transfer. Starred (*) and unstarred molecules represent enantiomers. (b) Unit-translated molecules in crystals of **11** where channels suitable for the propagation of the acyl transfer reaction are not available. These diagrams were generated using the packing diagrams obtained with the help of the program Mercury 3.8. Hydrogen atoms other than those of the hydroxyl groups are omitted for clarity.

orthoesters aided us in identifying key features in the crystal lattice that would support a facile intermolecular acyl transfer reaction. The results presented here demonstrate that analysis of intermolecular interactions and prior assessment of the molecular organization can be used as criteria for the rationalization and prediction of solid-state reactivity. Hence, we have been able to identify and predict the acyl transfer reactivity in co-crystals of naphthalene derivatives[8a] from a survey of the CSD, based on the results presented in this paper. It is important to note that the molecular structure of compounds used to arrive at the supramolecular structural criteria is very different from the constituents of the reactive crystal identified by survey of the CSD. The ability to identify molecular crystals capable of undergoing chemical reactions provides a practical alternative to designing reactive molecular crystals. The ability to predict the facility of reactions in molecular crystals is also important in view of the stability of crystals which play an important role in pharmaceutical solids,[12,22] synthetic inter-mediates,[23] and other supramolecular functional assemblies. This work also illustrates that an understanding of the structure of supramolecular assemblies is more relevant to explain observed reactivities and/or predict reactivity of small molecules rather than single molecular structures (as witnessed in 'organic reactive functional group' approach). This is evident from the fact that, although the single molecular structures of compounds in the present study varied widely, solids with comparable reactivity possess similar supramolecular features essential for facile solid-state acyl transfer reactivity.

■ EXPERIMENTAL SECTION

Racemic 2-O-Tosyl-4-O-benzoyl-*myo*-inositol 1,3,5-Orthoformate (8). Tosyl chloride (0.382 g, 2.0 mmol) was added to a solution of *myo*-inositol 1,3,5-orthoformate[24] (0.380 g, 2.0 mmol) in dry pyridine (5 mL), and the mixture was stirred for 12 h at room temperature. Benzoyl chloride (0.281 g, 2.0 mmol) was then added and stirring continued for another 12 h. Pyridine was evaporated under reduced pressure. Usual work up of the gum obtained in ethyl acetate followed by purification by silica gel column chromatography (gradient elution with light petroleum - ethyl acetate) gave the racemic **8** (0.584 g, 65%) as a colorless solid; it was crystallized from chloroform-light petroleum mixture. Mp 140−142 °C; IR (CHCl$_3$) $\bar{\nu}$ 1726, 3210−3472 cm^{-1}; ^{1}H NMR (200 MHz, CDCl$_3$) δ 2.36 (s, 3H), 2.77−2.80 (d, J = 5.3 Hz, 1H, D$_2$O exchangeable), 4.12−4.25 (m, 1H), 4.33−4.45 (m, 1H), 4.45−4.55 (m, 1H), 4.60−4.75 (m, 1H), 5.03−5.13 (m, 1H), 5.56 (s, 1H), 5.60−5.71 (m, 1H), 7.15−7.33 (m, 2H), 7.42−7.57 (m, 2H), 7.58−7.71 (m, 1H), 7.77−7.82 (d, J = 8.3 Hz, 2H), 7.92−7.98 (d, J = 8.3 Hz, 2H); ^{13}C NMR (CDCl$_3$, 125 MHz) δ 21.6, 67.3, 68.3, 69.4, 69.5, 72.1, 102.7, 127.8, 128.7, 129.8, 130.0, 133.8, 145.4, 164.7. Elemental analysis calcd for C$_{21}$H$_{20}$O$_9$S; C 56.25%, H 4.50%, found C 55.85%; H 4.56%.

General Procedure A: Acylation. Freshly distilled acid chloride was added to an ice-cooled solution of *myo*-inositol 1,3,5-orthofor-mate[24] in dry pyridine, with constant stirring. The reaction mixture was brought to room temperature, stirred for 18−20 h, and quenched with ice. Pyridine was removed under reduced pressure by co-evaporation with toluene (3 × 10 mL), and the residue was diluted with ethyl acetate and washed successively with water, 2% aqueous HCl, water, saturated sodium bicarbonate solution, and water followed by brine. The organic layer was dried over anhydrous sodium sulfate, and the solvent was evaporated under reduced pressure. The residue was flash chromato-graphed on silica using light petroleum-ethyl acetate (gradient elution).

Racemic 2,4(6)-Di-O-(p-iodobenzoyl)-*myo*-inositol 1,3,5-Or-thoformate (9). *myo*-Inositol orthoformate (0.190 g, 1 mmol) was acylated as described in the general procedure A with 4-iodobenzoyl chloride (~2 mmol) in dry pyridine (7 mL). The mixture of products obtained after workup was chromatographed to isolate racemic **9** (0.150 g, 23%). Crystallization of **9** from acetone, chloroform, nitromethane, 2-propanol or ethyl acetate yielded thin plate like crystals. Mp 240.3−

241.5 °C; IR (Nujol, cm^{-1}) $\bar{\nu}$ 3468, 1716; ^{1}H NMR (200 MHz, CDCl$_3$) δ 2.39 (1H, br s) 4.45−4.51 (1H, m), 4.55−4.65 (2H, m), 4.71−4.79 (1H, m), 5.60−5.66 (2H, m), 5.78−5.84 (1H, td, J = 4 and 1.7 Hz), 7.71−7.78 (2H, m), 7.80−7.88 (6H, m) ppm; ^{13}C NMR (50.3 MHz, CD$_3$COCD$_3$ + CD$_3$SOCD$_3$) δ 65.6, 67.5, 69.8, 69.9,70.4, 72.9, 102.2, 103.8, 130.3, 130.5, 132.2, 132.4, 138.9, 139.0, 165.6, 166.1 ppm; Elemental analysis calcd for C$_{21}$H$_{16}$O$_8$I$_2$: C, 38.80; H, 2.48. Found: C, 39.03; H,2.40%.

Racemic 2,4(6)-Di-O-(p-toluoyl) *myo*-inositol 1,3,5-Orthofor-mate (10) and 2-O-(p-Toluoyl)-*myo*-inositol 1,3,5-Orthoformate (11). *myo*-Inositol orthoformate (0.950 g, 5 mmol) was acylated as described in the general procedure A with p-toluoyl chloride (~11 mmol) in dry pyridine (12 mL). The products were separated by silica gel column chromatography to obtain racemic **10** (0.842 g, 39%) and **11** (0.630 g, 41%). Racemic **10** when crystallized from acetonitrile, acetonitrile-DCM, methanol, ethyl acetate, chloroform, dioxane, or nitromethane consistently yielded thin rectangular plates. Mp 227−229 °C; IR (Nujol, cm^{-1}) $\bar{\nu}$ 3473, 1720, 1716; ^{1}H NMR (200 MHz, CDCl$_3$) δ 2.41 (3H, s), 2.42 (3H, s) 2.59 (1H, br s), 4.45−4.53 (1H, m), 4.56−4.64 (2H, m), 4.68−4.77 (1H, m), 5.60−5.68 (2H, m), 5.83 (1H, td, J = 4 and 1.6 Hz), 7.20−7.31 (4H, m), 7.87−7.97 (2H, m), 7.99−8.08 (2H, m) ppm; ^{13}C NMR (50.3 MHz, CD3COCD3) δ 21.7, 65.0, 67.9, 69.5, 70.0, 70.7, 73.0, 103.9, 128.0, 128.3, 130.1, 130.2, 130.6, 130.8, 145.1, 166.4 ppm; Elemental analysis calcd for C$_{23}$H$_{22}$O$_8$: C, 64.78; H, 5.20. Found: C, 64.99; H, 4.80%.

The diol **11** when crystallized from acetone, ethyl acetate, chloroform, or dichloromethane yielded hexagonal plates. Mp 148−150 °C; IR (Nujol, cm^{-1}) $\bar{\nu}$ 3550−3350, 1703; ^{1}H NMR (200 MHz, CDCl$_3$): δ 2.05 (2H, br s), 2.42 (3H, s), 4.34−4.43 (1H, m), 4.43−4.53 (2H, m), 4.60−4.72 (2H, m), 5.50−5.62 (2H, m), 7.21−7.32 (2H, m), 7.97−8.08 (2H, m) ppm; ^{13}C NMR (50.3 MHz, CDCl$_3$): δ 21.7, 63.6, 68.0, 68.5, 71.9, 102.4, 126.4, 129.2, 130.0, 144.5, 166.9 ppm; Elemental analysis Calcd for C$_{15}$H$_{16}$O$_7$: C, 58.44; H, 5.23. Found: C, 58.52; H, 5.20%.

2,4,6-Tri-O-(p-toluoyl)-*myo*-inositol 1,3,5-Orthoformate (20). *myo*-Inositol orthoformate (0.190 g, 1 mmol) was acylated as described in the general procedure A with p-toluoyl chloride (~5 mmol) in dry pyridine (5 mL). The tri-p-toluate **20** (0.140 g, 26%) was isolated by column chromatography (silica gel). Mp 156−158 °C; IR (Nujol, cm^{-1}) $\bar{\nu}$ 1738, 1721; ^{1}H NMR (200 MHz, CDCl$_3$) δ 2.36 (6H, s), 2.44 (3H, s), 4.62−4.71 (2H, m), 4.94−5.03 (1H, m), 5.66−5.71 (1H, m),5.74 (1H, d, J 1.3 Hz), 5.78−5.86 (2H, m), 6.97 (4H, d, J = 8 Hz), 7.29−7.33 (2H, m), 7.66−7.77 (4H, m), 8.01−8.11 (2H, m) ppm; ^{13}C NMR (50.3 MHz, CDCl3) δ 21.6, 63.6, 66.9, 68.2, 69.4, 103.3, 125.7, 126.5, 128.9, 129.2, 129.8, 129.9, 144.1, 144.4,165.1, 166.2 ppm; Elemental analysis Calcd for C$_{31}$H$_{28}$O$_9$: C, 68.38; H, 5.18. Found: C, 68.07; H, 5.26%. The di-p-toluate **10** and p-toluic acid were also isolated as minor products.

Transesterification of Racemic 2-O-Tosyl-6-O-benzoyl-*myo*-inositol 1,3,5-Orthoformate (8) in its Crystals. The racemic benzoate **8** (0.200 g, 0.44 mmol) and Na$_2$CO$_3$ (0.379 g, 3.58 mmol, previously activated at 270 °C for 12 h) were ground together, and the mixture heated at 100 °C for 192 h. The reaction mixture turned black on heating. Analysis of this solid indicated the presence of 2-O-tosyl-4,6-di-O-benzoyl-*myo*-inositol 1,3,5-orthoformate, 2-O-tosyl-*myo*-inositol 1,3,5-orthoformate,[19] and the starting tosylate **8**. No attempt was made to purify these products since the yield was low.

Transesterification of Racemic 2,4(6)-Di-O-(p-iodobenzoyl)-*myo*-inositol 1,3,5-Orthoformate (9) in its Crystals. Crystals of **9** (0.0195 g, 0.03 mmol) and activated sodium carbonate (0.0254 g, 0.24 mmol) were ground together into a powder which was heated at 130 °C for 72 h. TLC analysis indicated a mixture of products, including **9** which were not separated.

Transesterification of Racemic 2,4(6)-Di-O-(p-methylbenzo-yl)-*myo*-inositol 1,3,5-Orthoformate (10) in its Crystals. Crystals of **10** (0.149 g, 0.35 mmol) and activated sodium carbonate (0.297 g, 2.8 mmol) were ground together into a powder which was initially heated at 110 °C for 17 h. TLC indicated the presence of only **10**. The temperature was increased up to 130 °C, and heating was continued for 47 h, at the end of which **10** was recovered quantitatively.

G

Transesterification of 2-O-(*p*-Methylbenzoyl)-*myo*-inositol 1,3,5-Orthoformate (11) in its Crystals. Crystals of **11** (0.047 g, 0.152 mmol, mp. 148−150 °C) were heated with Na_2CO_3 (0.150 g, 1.4 mmol) at 126 °C for 20 h; TLC of the reaction mixture showed the presence of the diester **10** and the triester **20**. The reaction mixture was loaded on a short silica gel (100−200 mesh) column and eluted with ethyl acetate (5 × 10 mL) and methanol (2 × 5 mL). The filtrate was concentrated, and the residue was chromatographed (230−400 mesh silica gel) by gradient elution with ethyl acetate−light petroleum mixture to obtain the triol **21** (0.012 g, 39%), the diester **10** (0.020 g, 29%), and the triester **20** (0.007 g, 8%). Other products present in trace amounts were not isolated.

■ ASSOCIATED CONTENT

ⓢ Supporting Information

The Supporting Information is available free of charge on the ACS Publications website at DOI: 10.1021/acs.joc.8b00293.

> Characterization data and ^1H and ^{13}C NMR spectra for all new products; single crystal X-ray diffraction data for **8**−**11**, ORTEPs and packing diagrams for **8**−**11** (PDF)
> Crystallographic data (CIF)

■ AUTHOR INFORMATION

Corresponding Author

*E-mail: ms.shashidhar@ncl.res.in. Fax: 91-20-25902629. Tel: 91-20-25902055.

ORCID ⓘ

Shobhana Krishnaswamy: 0000-0003-2479-2826

Mysore S. Shashidhar: 0000-0002-8477-1149

Present Address

†Department of Chemistry, Indian Institute of Technology, Madras, Chennai 600036

Notes

The authors declare no competing financial interest.

■ ACKNOWLEDGMENTS

■ REFERENCES

(1) Desiraju, G. R. *Angew. Chem., Int. Ed.* **2007**, *46*, 8342−8356.

(2) (a) Li, P.; He, Y.; Guang, J.; Weng, L.; Zhao, J. C.-G.; Xiang, S.; Chen, B. *J. Am. Chem. Soc.* **2014**, *136*, 547−549. (b) Black, H. T.; Perepichka, D. F. *Angew. Chem.* **2014**, *126*, 2170−2174.

(3) (a) Priimagi, A.; Cavallo, G.; Metrangolo, P.; Resnati, G. *Acc. Chem. Res.* **2013**, *46*, 2686−2695. (b) Gilday, L. C.; Robinson, S. W.; Barendt, T. A.; Langton, M. J.; Mullaney, B. R.; Beer, P. D. *Chem. Rev.* **2015**, *115*, 7118−7195. (c) Li, B.; Zang, S.-Q.; Wang, L.-Y.; Mak, T. C. W. *Coord. Chem. Rev.* **2016**, *308*, 1−21.

(4) Nishio, M.; Umezawa, Y.; Suezawa, H.; Tsuboyama, S. In *The Importance of π-Interactions in Crystal Engineering: Frontiers in Crystal Engineering*; Tiekink, E. R. T., Zukerman-Schpector, J., Eds.; Wiley-VCH: Chichester, UK, 2012; pp 1−39.

(5) Mann, L.; Voßnacker, P.; Müller, C.; Riedel, S. *Chem. - Eur. J.* **2017**, *23*, 244−249.

(6) (a) Chang, Y.; Chen, Y.; Chen, C.; Wen, Y.; Lin, J. T.; Chen, H.; Kuo, M.; Chao, I. *J. Org. Chem.* **2008**, *73*, 4608−4614. (b) Burattini, S.; Greenland, B. W.; Merino, D. H.; Weng, W.; Seppala, J.; Colquhoun, H. M.; Hayes, W.; Mackay, M. E.; Hamley, I. W.; Rowan, S. J. *J. Am. Chem. Soc.* **2010**, *132*, 12051−12058. (c) Bishop, R. In *The Importance of π-Interactions in Crystal Engineering: Frontiers in Crystal Engineering*; Tiekink, E. R. T., Zukerman-Schpector, J., Eds.; Wiley-VCH: Chichester, UK, 2012; pp 41−77.

(7) (a) Vyas, K.; Mohan Rao, V.; Manohar, H. *Acta Crystallogr., Sect. C: Cryst. Struct. Commun.* **1987**, *43*, 1197−1200. (b) Vyas, K.; Manohar, H.; Venkatesan, K. *J. Phys. Chem.* **1990**, *94*, 6069−6073. (c) Vyas, K.; Manohar, H. *Mol. Cryst. Liq. Cryst.* **1986**, *137*, 37−43.

(8) (a) Tamboli, M. I.; Krishnaswamy, S.; Gonnade, R. G.; Shashidhar, M. S. *Chem. - Eur. J.* **2013**, *19*, 12867−12874. (b) Tamboli, M. I.; Shashidhar, M. S.; Gonnade, R. G.; Krishnaswamy, S. *Chem. - Eur. J.* **2015**, *21*, 13676−13682 and references cited therein..

(9) (a) Ramamurthy, V.; Gupta, S. *Chem. Soc. Rev.* **2015**, *44*, 119−135. (b) Friščić, T.; MacGillivray, L. R. In *Making Crystals by Design - Methods, Techniques and Applications*; Braga, D., Grepioni, F., Eds.; Wiley-VCH: Weinheim, Germany, 2007; Chapter 2.3. (c) Huang, S.-L.; Hor, T. S. A.; Jin, G.-X. *Coord. Chem. Rev.* **2017**, *346*, 112−122. (d) Garcia-Garibay, M. A. *Acc. Chem. Res.* **2003**, *36*, 491−498. (e) Suzuki, M.; Fujii, T.; Naito, Y.; Yamoto, K.; Matsuoka, S.-I.; Takagi, K.; Sugiyama, H.; Uekusa, H. *Bull. Chem. Soc. Jpn.* **2018**, *91*, 343−348.

(10) (a) Blow, D. *Nature* **1990**, *343*, 694−695. (b) Brannigan, J. A.; Dodson, D.; Duggleby, H. J.; Moody, P. C. E.; Smith, J. L.; Tomchick, D. R.; Murzin, A. G. *Nature* **1995**, *378*, 416−419.

(11) Yang, C.; Xia, W. *Chem. - Asian J.* **2009**, *4*, 1774−1784.

(12) (a) Troup, A. E.; Mitchner, H. *J. Pharm. Sci.* **1964**, *53*, 375−379. (b) Jacobs, A. L.; Dilatush, A. E.; Weinstein, S.; Windheuser, J. J. *J. Pharm. Sci.* **1966**, *55*, 893−895. (c) Koshy, K. T.; Troup, A. E.; Duvall, R. N.; Conwell, R. N.; Shankle, L. L. *J. Pharm. Sci.* **1967**, *56*, 1117−1121. (d) Galante, R. N.; Visalli, A. J.; Patel, D. M. *J. Pharm. Sci.* **1979**, *68*, 1494−1498.

(13) (a) Biradha, K.; Santra, R. *Chem. Soc. Rev.* **2013**, *42*, 950−967. (b) Bürgi, H. B.; Dunitz, J. D. *Acc. Chem. Res.* **1983**, *16*, 153−161.

(14) Coley, C. W.; Barzilay, R.; Jaakkola, T. S.; Green, W. H.; Jensen, K. F. *ACS Cent. Sci.* **2017**, *3*, 434−443.

(15) Devaraj, S.; Shashidhar, M. S.; Dixit, S. S. *Tetrahedron* **2005**, *61*, 529−536.

(16) Krishnaswamy, S.; Gonnade, R. G.; Shashidhar, M. S.; Bhadbhade, M. M. *CrystEngComm* **2010**, *12*, 4184−4197.

(17) (a) Praveen, T.; Samanta, U.; Das, T.; Shashidhar, M. S.; Chakrabarti, P. *J. Am. Chem. Soc.* **1998**, *120*, 3842−3845. (b) Sarmah, M. P.; Gonnade, R. G.; Shashidhar, M. S.; Bhadbhade, M. M. *Chem. - Eur. J.* **2005**, *11*, 2103−2110. (c) Murali, C.; Shashidhar, M. S.; Gonnade, R. G.; Bhadbhade, M. M. *Eur. J. Org. Chem.* **2007**, *2007*, 1153−1159. (d) Murali, C.; Shashidhar, M. S.; Gonnade, R. G.; Bhadbhade, M. M. *Chem. - Eur. J.* **2009**, *15*, 261−269.

(18) Nishio, M.; Umezawa, Y.; Honda, K.; Tsuboyama, S.; Suezawa, H. *CrystEngComm* **2009**, *11*, 1757−1788.

(19) Sureshan, K. M.; Shashidhar, M. S.; Praveen, T.; Gonnade, R. G.; Bhadbhade, M. M. *Carbohydr. Res.* **2002**, *337*, 2399.

(20) Riley, A. M.; Mahon, M. F.; Potter, B. V. L *Angew. Chem., Int. Ed. Engl.* **1997**, *36*, 1472−1474.

(21) (a) MacGillivray, L. R. *J. Org. Chem.* **2008**, *73*, 3311−3317. (b) MacGillivray, L. R.; Papaefstathiou, G. S.; Friščić, T.; Hamilton, T. D.; Bucar, D.; Chu, Q.; Varshney, D. B.; Georgiev, I. G. *Acc. Chem. Res.* **2008**, *41*, 280−291. (c) Natarajan, A.; Bhogala, B. R. In *Bimolecular Photoreactions in the Crystalline State, in Supramolecular Photochemistry: Controlling photochemical processes*, Ramamurthy, V., Inoue, Y., Eds.; John Wiley & Sons: Hoboken, NJ, 2011; pp 175−228.

(22) (a) Cheng, Y.-D.; Lin, S.-Y. *J. Agric. Food Chem.* **2000**, *48*, 631−635. (b) Wang, S.-L.; Lin, S.-Y.; Chen, T.-F. *Chem. Pharm. Bull.* **2001**, *49*, 402−406. (c) Hsu, C.-H.; Lin, S.-Y. *Thermochim. Acta* **2009**, *486*, 5−10.

(23) Sardessai, R.; Krishnaswamy, S.; Shashidhar, M. S. *CrystEngComm* **2012**, *14*, 8010−8016.

(24) Uhlmann, P.; Vasella, A. *Helv. Chim. Acta* **1992**, *75*, 1979−1994.